The Geological Society

ES3 Earth Science, Systems and Society

ORIGINAL RESEARCH
published: 25 September 2024
doi: 10.3389/esss.2024.10126

Origin and Affinities of the Malmberget Iron Oxide-Apatite Deposit, Northern Sweden: Insights From Magnetite Chemistry and Fe-O Isotopes

Jens S. Henriksson[1,2†], Valentin R. Troll[1*†], Ellen Kooijman[3], Ilya Bindeman[4], Tomas Naeraa[5] and Tobias E. Bauer[6]

[1]Section for Natural Resources and Sustainable Development, Department of Earth Sciences, Uppsala University, Uppsala, Sweden, [2]Exploration Department, Luossavaara Kiirunavaara Aktiebolag, Malmberget, Sweden, [3]Department of Geosciences, Swedish Museum of Natural History, Stockholm, Sweden, [4]Stable Isotope Laboratory, Department of Earth Sciences, University of Oregon, Eugene, OR, United States, [5]Department of Geology, Lund University, Lund, Sweden, [6]Division of Geosciences and Environmental Engineering, Luleå University of Technology, Luleå, Sweden

OPEN ACCESS

Edited by:
Albertus Smith,
University of Johannesburg, South Africa

Reviewed by:
Fernando Tornos,
Spanish National Research Council (CSIC), Spain
Shengchao Yan,
Institute of Geology and Geophysics (CAS), China

***Correspondence**
Valentin R. Troll,
valentin.troll@geo.uu.se

[†]These authors have contributed equally to this work

Received: 12 April 2024
Accepted: 27 August 2024
Published: 25 September 2024

Citation:
Henriksson JS, Troll VR, Kooijman E, Bindeman I, Naeraa T and Bauer TE (2024) Origin and Affinities of the Malmberget Iron Oxide-Apatite Deposit, Northern Sweden: Insights From Magnetite Chemistry and Fe-O Isotopes. *Earth Sci. Syst. Soc.* 4:10126. doi: 10.3389/esss.2024.10126

European iron ore production is primarily sourced from magnetite dominated iron oxide-apatite ore deposits in the northern Norrbotten ore province of northernmost Sweden. The Malmberget iron oxide-apatite deposit is at present the largest iron ore resource in Europe and is an amphibolite facies grade analogue of the world-famous Kiirunavaara iron oxide-apatite deposit. The Malmberget rock association is characterised by multiple phases of deformation, metamorphism, and alteration that resulted in a geometrically and petrologically complex deposit that is genetically ambiguous. Primary ore textures and emplacement structures of the Malmberget iron oxide-apatite deposit have largely been recrystallised during metamorphic overprinting and now comprise dominantly medium- to coarse-grained granoblastic magnetite. However, isotopic characteristics are preserved and when combined with trace element chemistry, these can be used to understand magmatic vs. hydrothermal origin of the deposit. To unravel the primary origin of the Malmberget magnetite ore, we combined magnetite trace element chemistry and Fe-O stable isotopes to investigate the massive magnetite in the Fabian-Kapten and ViRi ore bodies of the Malmberget iron oxide-apatite deposit. Trace element correlations indicate a high-temperature magmatic to a transitional high-temperature magmatic-hydrothermal origin of the Malmberget iron oxide-apatite ore deposit, with data plotting into fields of clear magmatic affinity in trace element discrimination diagrams. Fe-O data fall into established magmatic fields regardless of subsequent metamorphic modifications, underlining a dominantly (ortho-)magmatic origin of the investigated deposits. Despite an overall magmatic to magmatic-hydrothermal origin for the two ore bodies studied, Fe-O isotope equilibrium calculations of the magnetite suggest a possible temperature discrepancy between the Fabian-Kapten ore body and the ViRi ore body, the latter showing a more

pronounced magmatic character. These variations in trace element contents and Fe-O isotopes can be explained by the proximity of the more magmatic signatures to the centre of the ore forming magmatic system.

Keywords: Malmberget ore deposit, magnetite chemistry, IOA, Fe-O, stable isotopes

INTRODUCTION

Iron has been a driver of industrial revolution and remains the most important metal for the modern industry and will remain so for the foreseeable future (U.S. Geological Survey, 2023). It is widely used in civil engineering, manufacturing, transport, and as a catalyst in chemical processing. The EU's iron ore production is to over 80% sourced from Kiruna-type Iron Oxide-Apatite (IOA) deposits located in the northern Norrbotten ore province in northern Sweden (SGU, 2023; LKAB, 2024), which hosts several large IOA deposits. Iron oxide apatite deposits are usually modally dominated by magnetite, with variable amounts of hematite, apatite, actinolite, diopside and possibly accessory phases such as monazite or xenotime. In northern Sweden, the main iron ore sources are the Kiirunavaara and Malmberget deposits, which together with Svappavaara constitute the biggest IOA deposits in the region (Bergman et al., 2001; Martinsson et al., 2016). The Malmberget IOA deposit is considered an amphibolite facies equivalent of the world famous Kiirunavaara IOA deposit (Geijer, 1930; Annersten, 1968; Bergman et al., 2001; Yan et al., 2023a) and represents the largest iron ore resource in Europe. It is estimated at ca. 2 Gt, whereas Kiirunavaara is currently listed at ca.1.5 Gt (LKAB, 2024).

Formation of IOA deposits is usually related to convergent margin tectonics and associated calc-alkaline magmatism or to post-collisional periods of extensional tectonics associated with somewhat alkaline magmatism (Witschard, 1984; Martinsson and Perdahl, 1995; Majidi et al., 2021; Andersson et al., 2021). The principal formation mechanism of giant-sized IOA deposits remains ambiguous, and is surrounded by an intense scientific debate, both historically (cf. Geijer, 1910; Parák, 1975; Naslund, 1983 Hildebrand, 1986; Hitzman et al., 1992; Nyström and Henríquez, 1994; Naslund et al., 2002; Jonsson et al., 2013), and more recently (Dare et al., 2014; Tornos et al., 2016; 2017; 2024; Westhues et al., 2017; Simon et al., 2018; Troll et al., 2019; Peters et al., 2020; Reich et al., 2022; Yan and Liu, 2022). Recent studies on trace elements, fluid inclusions, and stable and radiogenic isotopes have progressed the understanding of IOA deposits, both on a deposit-to-regional scale and on a global scale, and suggest that IOA deposits dominantly form from magmatic processes, although no single model on the exact formation mechanisms has been derived to date (Westhues et al., 2017; Troll et al., 2019; Peters et al., 2020; Rodriguez-Mustafa et al., 2020; Reich et al., 2022; Pietruszka et al., 2023, 2024; Tornos et al., 2024).

In natural systems, magnetite cation substitution commonly occurs in both the tetrahedral (Fe^{3+}) and octahedral sites (Fe^{2+}, Fe^{3+}), with the concentration and preferred cation being dependant on temperature, pressure, ionic radius and charge, with the latter being dependant on oxygen fugacity (Toplis and Corgne, 2002; Nadoll et al., 2014; Sievwright et al., 2017). Cation incorporation is theoretically limited to monovalent (Cu^{+}), divalent (Mg^{2+}, Ti^{2+}, V^{2+}, Cr^{2+}, Mn^{2+}, Co^{2+}, Ni^{2+}, Zn^{2+}, Ge^{2+}), trivalent (Mg^{3+}, Al^{3+}, Sc^{3+}, Ti^{3+}, V^{3+}, Cr^{3+}, Mn^{3+}, Co^{3+}, Ni^{3+}, Zn^{3+}, Ge^{3+}, As^{3+}, Nb $^{3+}$, Mo^{3+}, Ta^{3+}) and tetravalent cations (Ti^{4+}, V^{4+}, Nb^{4+}, Mo^{4+}, Sn^{4+}, Ta^{4+}, W^{4+}) to maintain isomorphic substitution (Nadoll et al., 2014 and references therein). During the two last decades, trace element contents in magnetite have been studied and applied to constrain petrogenetic factors for a wide range of ore deposit types (i.e., Dupuis and Beaudoin, 2011; Dare et al., 2014; Nadoll et al., 2014; Wen et al., 2017). These diagrams have been applied to distinguish magnetite populations in individual deposits, and to compare trace element signatures of different deposits. Notable examples applied to IOA deposits are conducted by Knipping et al. (2015), Ovalle et al. (2018), Palma et al. (2021), Duan et al. (2019), Salazar et al. (2020) and Ye et al. (2023). Tornos et al., 2024 recently raised concerns regarding the limitations and uncertainties that arise when empirically derived trace element discrimination diagrams are used on a global scale to classify ore deposits and estimate formation temperatures, without precise geochemical and petrogenetic constraints. Here we use trace element data from magnetite as a first order assessment tool and combine the results with stable isotope studies of Fe and O to evaluate potential geochemical differences between the Fabian-Kapten and ViRi ore bodies.

Recent stable isotope thermometry and tracer studies, using δ^{56}Fe- and δ^{18}O-isotopes (Fe-O isotopes) on IOA deposits, have allowed to advance discussion on primary origins of IOA ores and suggest a predominately high-temperature, and thus magmatic to magmatic-hydrothermal, origin (>800˚C) (Jonsson et al., 2013; Bilenker et al., 2016; Simon et al., 2018; Troll et al., 2019; Childress et al., 2020). This is possible because the large volumes of magnetite buffer the system with regards to post-depositional reequilibration of the Fe-O composition. The common small volumes of locally associated low-temperature hydrothermal magnetite are generally attributed to a progressively cooling magmatic system influenced by dissolution and replacement precipitation due to interaction with low-temperature hydrothermal and meteoric fluids (e.g., Bilenker et al., 2016; Simon et al., 2018; Troll et al., 2019; Reich et al., 2022).

It is notable that trace element and Fe-O isotope data for the Malmberget deposit was limited or absent. The magnetite composition was previously analysed in a doctoral and an MSc thesis using EPMA (Lund, 2013; Kambai, 2021), and two oxygen isotope values were reported in an MSc thesis by Lund (2014). However, the lack of high-resolution trace element data

and the absence of correlated Fe-O constraints limits the understanding of ore formation at this major deposit, which hampers comparisons between the Malmberget deposit and other IOA deposits in the region, such as the famous Kiruna deposits. In addition, the understanding of magnetite trace element redistribution and Fe-O isotope partitioning under medium- to high-grade metamorphism of IOA deposits is limited (Reich et al., 2022).

Here we present new trace element and Fe-O isotope data from massive magnetite samples from two ore bodies of the Malmberget IOA deposit to shed light on deposit-scale differences and its primary origin to allow comparison with other IOA deposits worldwide. We evaluate to what extent the amphibolite facies metamorphism in the Malmberget area has affected the trace element distribution and magnetite Fe-O isotope composition of the deposit, with the intent to expand the current understanding of chemical and isotopic partitioning during metamorphic process in IOA deposits. In particular, we test if trace element and stable isotope characteristics of magnetite can sustain metamorphic overprinting and establish if the Malmberget deposit is primarily of magmatic or of hydrothermal origin. This will help to further resolve the prime controversy on the origin of IOA ores that has been ongoing for many decades (cf. Simon et al., 2018; Troll et al., 2019; Reich et al., 2022).

GEOLOGICAL BACKGROUND

The Malmberget IOA deposit is located 5 km north of Gällivare town in Norrbotten county in northernmost Sweden (**Figures 1A–C**). It is the second largest underground iron mine in the world, second to the Kiruna mine and the current annual production amounts to 19 Mt at 39.4 Fe wt.% (LKAB, 2024). The country rocks to the IOA ore in the Norrbotten ore province are dominated by variably deformed and metamorphosed Paleoproterozoic igneous and sedimentary rocks formed in a back-arc environment during the 2.0–1.75 Ga Svecofennian orogeny (Martinsson and Perdahl, 1995; Bergman et al., 2001; Sarlus et al., 2018; Bergman and Weihed, 2020).

The Malmberget IOA deposit (**Figure 1C**) is hosted in a 1.89–1.88 Ga volcano-sedimentary succession comprising mafic to felsic metavolcanic rocks that have been intruded by multiple generations of granites, pegmatites, and dolerite dykes (Lund, 2013; Sarlus et al., 2020). The largest intrusive unit belongs to the Lina granite-pegmatite suite and borders the ore deposit to the north and northwest.

The Svecofennian rocks, which host the IOA deposits, are underlain by Archean rocks. The northern part of the northern Norrbotten ore province is underlain by early Paleoproterozoic (2.4–2.1 Ga), pre-orogenic green stone belts (Gaál and Gorbatschev, 1987; Martinsson, 1997; Hanski and Huhma, 2005). In the province's westernmost segment, the Precambrian basement is overlain by Ediacaran to Cambrian metasedimentary rocks, which have been overthrusted by Caledonian nappes (Bergman et al., 2001). The Svecofennian supracrustal rocks can be divided into three stratigraphic groups: the Kurravaara conglomerate and the Porphyrite group (1.91–1.88 Ga), the Kiirunavaara group (sometime referred to as the Porphyry group; 1.89–1.87 Ga), and the Hauki group (<1.88 Ga) (Martinsson et al., 2016; Bergman and Weihed, 2020). The Malmberget and the Kiirunavaara IOA deposits are both hosted within the Kiirunavaara group, which comprises mildly alkaline, bimodal volcanic rocks and can be distinguished from the Porphyrite group volcanic rocks based on Ti and Zr contents (Martinsson and Perdahl, 1995). The Kiirunavaara group rocks are considered comagmatic with the Perthite monzonite intrusive suite, and were presumably emplaced in an extensional tectonic environment, possibly influenced by plume activity (Martinsson and Perdahl, 1995; Sarlus et al., 2018, 2020). Late Svecokarelian intrusive suites cover large areas of northern Norrbotten and comprise the Edefors suite with Transscandinavian igneous belt supersuite affinity and late to post-collisional granites belonging to the Lina granite-pegmatite suite (e.g., Andersson, 1991; Högdahl et al., 2004; Sarlus et al., 2018).

U-Pb radiometric age determination of zircon from the Kiirunavaara ore constrain IOA deposit formation in the Norrbotten region to between 1.88 and 1.87 Ga (Westhues et al., 2017). U-Pb radiometric age determination of oscillatory zoned zircon grains from the metavolcanic host rocks in Malmberget yield magmatic ages between 1.89 and 1.87 Ga, which thus overlap with ore formation age. Subsequent metamorphic overprint was dated at between 1.80 and 1.77 Ga (Sarlus et al., 2018; Sarlus et al., 2020). In line with this, recent U-Pb radiometric age determination of the Malmberget apatite seems to confirm amphibolite-facies (≥550°C) recrystallisation and homogenisation at around 1.80 Ga and suggest an igneous source of the apatite based on Sr isotope signatures and trace element patterns (Yan et al., 2023a).

Magnetite is the primary iron-oxide ore mineral, but mixed magnetite-hematite ore and pure hematite ore occur locally. The ore and side-rock in the Gällivare-Malmberget area are characterised by multiple events of alteration, deformation and metamorphism that have overprinted primary textures and features of both host rock and ore, with peak metamorphism reaching amphibolite facies conditions (Annersten, 1968; Bergman et al., 2001; Martinsson et al., 2016; Bauer et al., 2018; Yan et al., 2023a).

Four phases of deformation are recognised in the Gällivare-Malmberget area, two ductile (D_1, D_2) and two brittle (D_3, D_4). The first deformation phase (D_1) resulted in formation of a penetrative tectonic fabric during regional metamorphism around 1.87–1.86 Ga (Bauer et al., 2018, 2022). The second deformation event around 1.80–1.78 Ga (D_2) caused folding of the originally continuous, bedding parallel ore-bearing volcano-sedimentary package as well as the S_1-fabric into a large-scale, SW-plunging synform under brittle-plastic conditions (Geijer, 1930; Martinsson et al., 2016; Bauer et al., 2018; Andersson et al., 2021). During metamorphism and/or deformation secondary lithologies formed; biotite schist formed due to strain partitioning between ore and host rock during

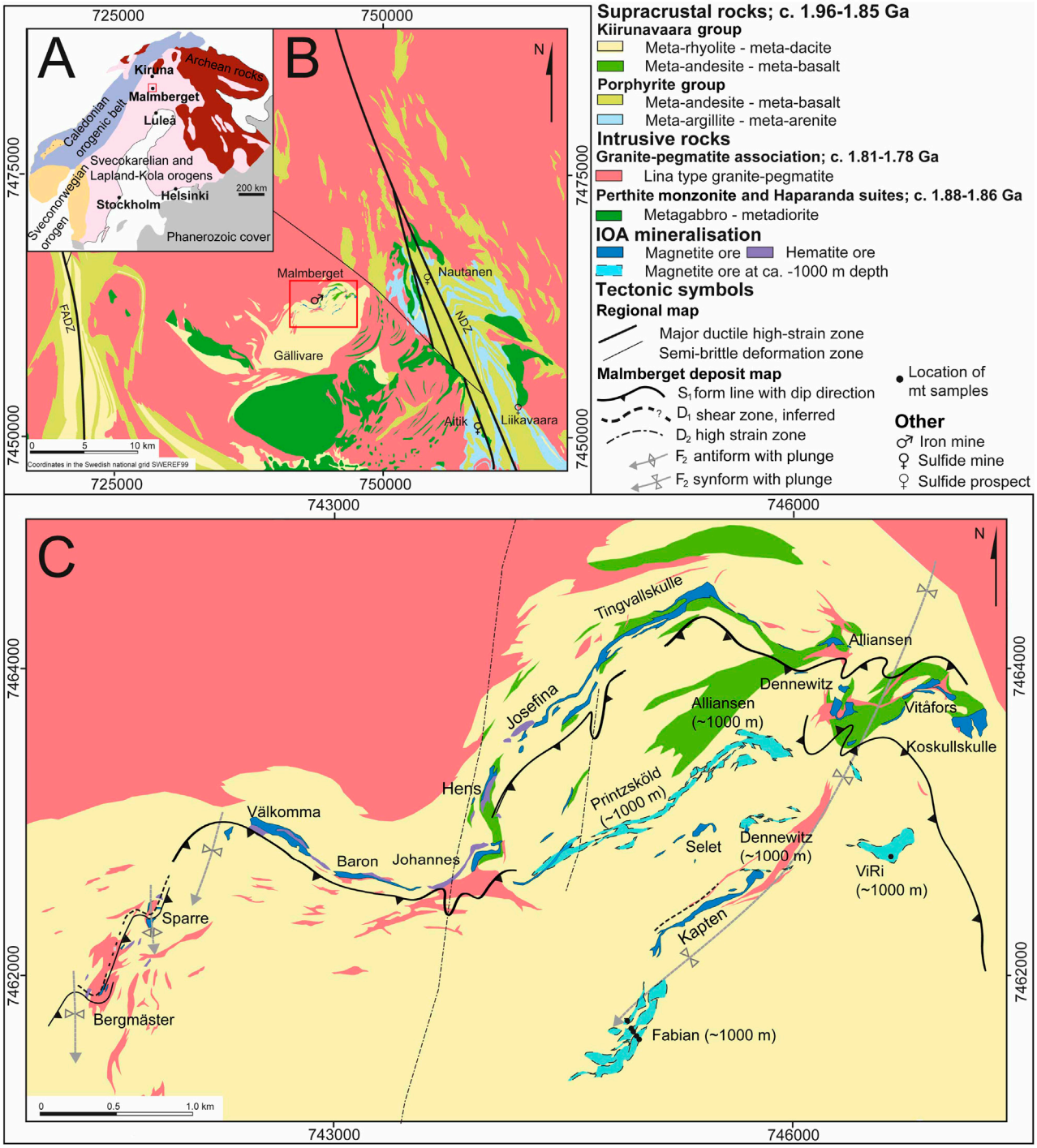

FIGURE 1 | (A) Generalised geological map of the Fennoscandian Shield. The red rectangle highlights the area shown in image **(B)**; NDZ, Nautanen deformation zone; FADZ, Fjällåsen Allavara deformation zone. **(B)** geological map of the Gällivare-Malmberget area with the red rectangle highlighting the are shown in **(C)**; **(C)** geological map of the Malmberget IOA deposit with structural interpretation from Bauer et al. (2018). Modified from Geijer (1930); Lund (2013); Bauer et al. (2018).

shearing, and sillimanite-bearing gneisses formed as a result of contact metamorphism caused by the intruding Lina granite-pegmatite suite at around 1.80 Ga. D3 structures comprises brittle faults and fractures, and D4 structures consist of open, clay-, chlorite-, and epidote-filled fractures (Bauer et al., 2018). U-Pb dating of monazite and titanite in stilbite-bearing assemblages constrains the D4 event between 1.74 and 1.60 Ga, and U-Pb and Pb-Pb of stilbite indicate ambient

temperatures in the Malmberget area below 150°C after 1.73 Ga (Romer, 1996).

Lund (2013) suggested that the Malmberget ore is hosted in three different stratigraphic positions, where the Fabian-Kapten and ViRi ore bodies sit at the lowest position, Printzsköld-Alliansen at the middle position, and the Välkomma, Baron, Johannes and Hens-Josefina, collectively referred to as the Western field ores sit at the highest position. On the contrary, Bauer et al. (2018) interpreted at least two stratigraphic positions of the ore from structural data. In their model, the stratigraphically lower ore position forms a ca. 5 km semi-continuous ore zone, from the Western field through Printzsköld-Alliansen to Östergruvan, Dennewitz, Parta and ViRi in the east, whereas the stratigraphically upper ore position comprises the Fabian-Kapten ore body, situated in the fold hinge of the Malmberget synform.

In this study, we provide trace element compositions and Fe-O isotope signatures of massive magnetite samples from two ore bodies within the Malmberget IOA deposit. Magnetite trace element contents and Fe-O isotope signatures are compared to regional and global IOA deposits with the aim to test whether Fe-O systematics can unequivocally discern the primary magnetite source for the metamorphically overprinted (amphibolite facies) Malmberget IOA deposits. In addition, we test if deposit-scale variations in magnetite trace element contents and isotope composition exist in the two ore bodies in order to investigate if a larger geochemical study of the Malmberget IOA deposit will be a feasible approach to help further unravel the stratigraphic positions of individual ore bodies within the overall deposit.

SAMPLES AND METHODS

Six massive magnetite samples were collected from one drill core transecting the Fabian-Kapten ore body (N = 5) and one drill core transecting the ViRi ore body (N = 1), at depths of −1,550 m and −1,220 m, respectively (**Figure 1C**). Epoxy mounts were prepared from each sample for SEM and for LA-ICPMS analysis.

In preparation for Fe-O isotope analysis, the massive magnetite samples were crushed and magnetically separated at Uppsala University. Individual magnetite grains were then inspected and hand-picked under a stereomicroscope to ensure purity and only pristine crystals were selected for isotope analysis.

SEM-imaging for textural analysis was conducted at LKAB Malmberget, Sweden, using a FEI Quanta FEG 650 SEM. The voltage of the accelerating electron beam was set to 10 kV and the working distance was ~130 mm.

EBSD-imaging was performed at the Swedish Museum of Natural History. The results presented here were previously reported in the first authors MSc thesis (Henriksson, 2022). We used an Oxford Instruments Nordlys detector attached to a FEI Quanta FEG 650 SEM, based on the procedure outlined in Kenny et al. (2020), using magnetite match units from Wechsler et al. (1984). Data collection and post-acquisition processing was done using the software's Aztec and Channel 5 from Oxford Instruments.

Concentrations of Mg^{24}, Mg^{25}, Al^{27}, Sc^{45}, Ti^{49}, V^{51}, Cr^{52}, Mn^{55}, Co^{59}, Ni^{60}, Zn^{66}, Ga^{71}, and Sn^{118} in magnetite were measured at the Laser Ablation Inductively Coupled Mass Spectrometry (LA-ICP-MS) laboratory at Lund University, Sweden. The laboratory hosts a Teledyne Photon Machines G2 laser coupled to a Bruker Aurora Elite quadrupole ICP–MS. The laser is equipped with a HelEx 2-volume sample cell. All analyses were conducted with a 25 µm spot size using a scan time of 30 s. The carrier gas (He 0.8 L/min) was mixed with Ar (0.95 L/min) downstream of the sample chamber. ICP-MS tuning was done with NISTSRM612 in normal sensitivity mode and it was aimed at obtaining stable signal counts on relevant isotopes, with oxide production below 0.5% monitoring $^{238}U/^{238}U^{16}O$ and $^{232}Th/^{232}Th^{16}O$, and on Th/U ratios around 1. The external standard BCR-2G was used for calibration and BHOV-2G was analysed as secondary standard, both are basaltic glasses from USGS (Jochum et al., 2005). Fe^{57} was used as an internal standard. Standard-sample-standard bracketing was applied for drift correction and quantification. Data reduction was done using the X_Trace_Elements_IS data reduction scheme (DRS) in Iolite (Woodhead et al., 2007; Paton et al., 2011).

The magnetite separates were analysed for the stable isotope ratios $\delta^{56}Fe$ and $\delta^{18}O$. The isotope ratios were previously reported in the first author's MSc thesis and a conference contribution (Henriksson, 2022; Henriksson et al., 2023).

Oxygen (O) isotope analysis was performed at the University of Oregon following the procedure described in Bindeman et al. (2022). A MAT 253 gas isotope ratio mass spectrometer with a fluorination line attached, in dual inlet mode was used for oxygen isotope analysis. BrF_5 was used as a reagent to liberate oxygen from the magnetite crystals. The oxygen gas extracted from minerals in the laser chamber was purified through a series of cryogenic traps at liquid nitrogen temperature and a mercury diffusion pump to freeze reaction products and excess of F_2 gas generated during fluorination. A platinum-graphite converter was used to convert Oxygen to CO_2 gas. An in-house Gore Mountain garnet standard (UOG, +6.52‰) was used for calibration before and after analysis of the magnetite samples, alongside with UWG-2 standard (+5.8‰, Valley et al., 1995). The values obtained for the UOG garnet standard were +6.54‰ and +6.40‰. Oxygen isotope values are reported relative to the Standard Mean Ocean Water (SMOW). The average external reproducibility (2σ) of $\delta^{18}O$ was 0.2‰.

Iron (Fe) isotope analysis was conducted at the Vegacenter at the Swedish Museum of Natural History in Stockholm using a Nu Plasma II HR-MC-ICP-MS in pseudo-high-resolution mode. Prior to analysis the magnetite crystals were digested and purified in concentrated HF, HNO_3 and 10M HCl following the procedures described in (Borrok et al., 2007; Millet et al., 2012). Subsequently, the samples were diluted with 0.3M HNO_3 to a concentration of 2–3 ppm. All values were corrected for mass bias and are reported relative to IRMM-014 from Isotopic

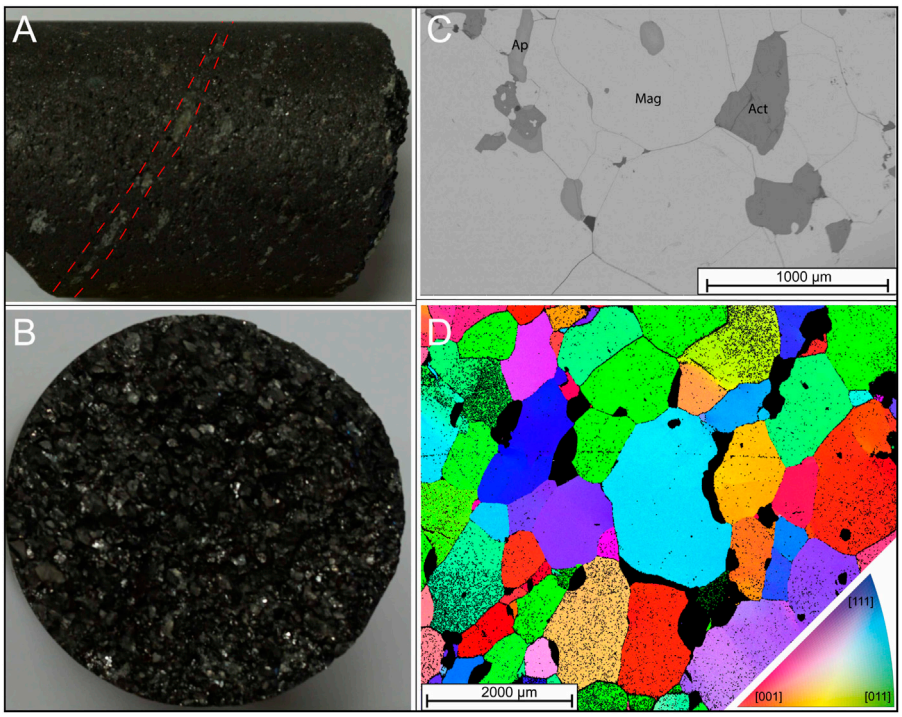

FIGURE 2 | Representative-images of the analysed samples. **(A, B)** photographs of sample FA-001 that consist of medium- to coarse-grained massive magnetite with foliated apatite grains. The diameter of the drill core is 3.90 cm; **(C)** BSE-image of FA-001 comprising magnetite, minor apatite and actinolite; **(D)** EBSD-image of sample FA-001 showing magnetite crystal orientations. Note granoblastic textures with clear triple junctions and sub-grain domains. Black pixels represent a non-indexed or non-magnetite phase.

Reference Materials and Measurements (Brand et al., 2014). The average external reproducibility (2σ) for δ^{56}Fe was 0.07‰.

RESULTS

The ore textures in the massive magnetite samples from the Malmberget IOA deposit are to a large degree recrystallised, exhibiting granoblastic intergranular relationships with distinct triple junctions (cf. Jonsson et al., 2016). In addition to magnetite, the ore assemblage can also include subordinate amounts of interstitial fluorapatite and silicates such as biotite, actinolite, tremolite and diopside.

The granoblastic texture is a characteristic feature for well-equilibrated metamorphic assemblages that indicates equilibration over extended time frames (**Figures 2A–D**). This is consistent with previously established amphibolite facies metamorphism (Annersten, 1968), as well as homogenisation of U-Pb in apatite at around 1.80 Ga (Yan et al., 2023a).

Magnetite Chemistry

Magnetite trace element concentrations have been analysed for samples FA-KA-001 and ViRi-001. In total, 24 points were analysed, 12 for each sample. All Cr analyses, and a significant amount of the Sc and Zn analyses were below the detection limit (**Figure 3**; **Supplementary Table S1**). The Fabian-Kapten magnetite grains have average Mg, Al, Sc, Ti, V, Mn, Co, Ni, Zn, Ga, and Sn contents of 2,951 ppm, 1,341 ppm, 3 ppm, 530 ppm, 1,047 ppm, 366 ppm, 73 ppm, 164 ppm, 17 ppm, 34 ppm, and 1 ppm, respectively. The magnetite grains from the ViRi ore body have average Mg, Al, Sc, Ti, V, Mn, Co, Ni, Zn, Ga, and Sn contents of 533 ppm, 1,277 ppm, 3 ppm, 4,477 ppm, 1,967 ppm, 238 ppm, 63 ppm, 169 ppm, 15 ppm, 52 ppm, and 1 ppm, respectively (**Figures 3**, **4**). The most noticeable discrepancies in magnetite trace element contents between the Fabian-Kapten and ViRi ore bodies can be observed for Mg, Ti, V, Mn, Co, and Ga. The Fabian-Kapten magnetite shows comparably elevated contents relative to the ViRi magnetite in Mg (avg. 2,951 vs. 533 ppm), Mn (avg. 366 vs. 238 ppm), and Co (avg. 73 vs. 63 ppm). In contrast, Fabian-Kapten magnetite displays lower trace element contents relative to the ViRi magnetite in Ti (avg. 530 vs. 4,477 ppm), V (avg. 1,047 vs. 1,967 ppm), and Ga (avg. 34 vs. 52 ppm). The average vanadium content in the Fabian-Kapten (1,047 ppm) and the ViRi (1,967 ppm) bodies is distinctly different. However, the vanadium values within each ore body are completely uniform, with standard deviations of 7 ppm for the Fabian-Kapten ore body and 27 ppm for the ViRi body.

Fe-O Isotopes

The obtained Fe-O isotope values for massive magnetite samples from the Fabian-Kapten and ViRi ore bodies of the Malmberget IOA deposit (**Supplementary Table S1**) show a δ^{18}O isotope range between +1.1‰ and +3.7‰ (**Figure 5**), and a

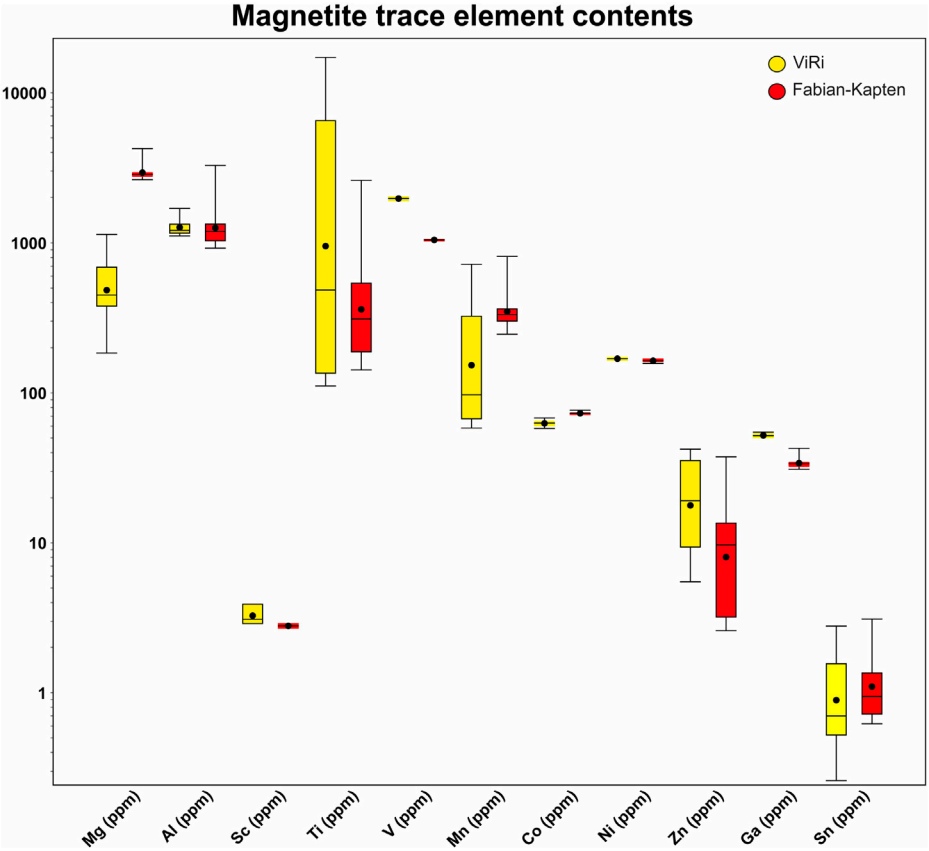

FIGURE 3 | Box and whisker plots for trace elements in magnetite. Lines show the median values and solid black circles show mean values. The central box represents the middle 50% of the data (Q1 to Q3). Whiskers represents the range Q3-Q1*<1.5.

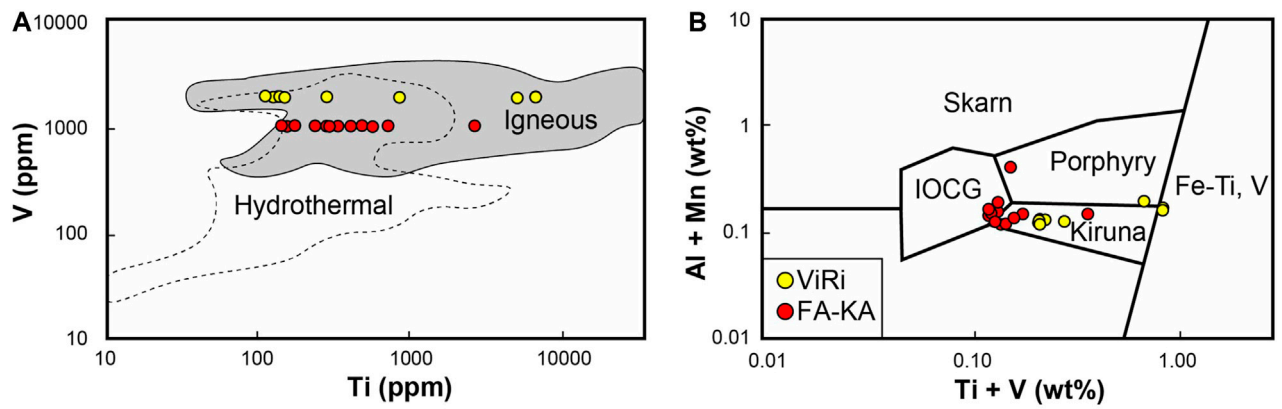

FIGURE 4 | Magnetite trace element discrimination diagrams. **(A)** Ti vs. V concentrations in magnetite. Fields based on data from Nadoll et al. (2014); **(B)** Ti + V vs. Al + Mn concentrations in magnetite. Fields from Dupuis and Beaudoin (2011).

δ^{56}Fe isotope range between +0.16‰ and +0.25‰ (**Figure 6**). The five massive magnetite samples from the Fabian-Kapten ore body have δ^{18}O values between +1.1‰ and +3.7‰, and δ^{56}Fe values between +0.16‰ and +0.19‰. The sample from the ViRi ore body has a δ^{18}O value of +1.7‰, and a δ^{56}Fe value of +0.25‰. Thus the Viri ore body falls into the range of values for oxygen determined for the Fabian-Kapten samples, but exceeds the Fe isotope range for the Fabian-Kapten samples, implying that there is a genetic difference. Both δ^{18}O and δ^{56}Fe isotope values, however, overlap with the established literature ranges for igneous magnetite (see discussion below).

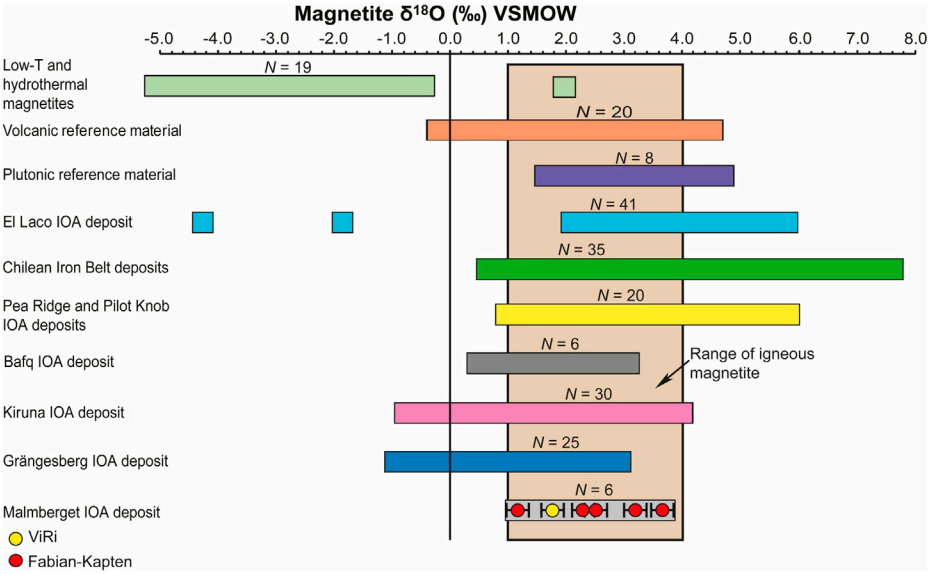

FIGURE 5 | Discriminant diagram for oxygen isotopes signatures in magnetite. The coloured fields correspond to the range of $\delta^{18}O$ isotopes for magnetite reported in Bilenker et al. (2016), Childress et al. (2016), Loewen and Bindeman (2016), Troll et al. (2019), Rodriguez-Mustafa et al. (2020) and Xie et al. (2021). Range of igneous magnetite from Taylor (1967).

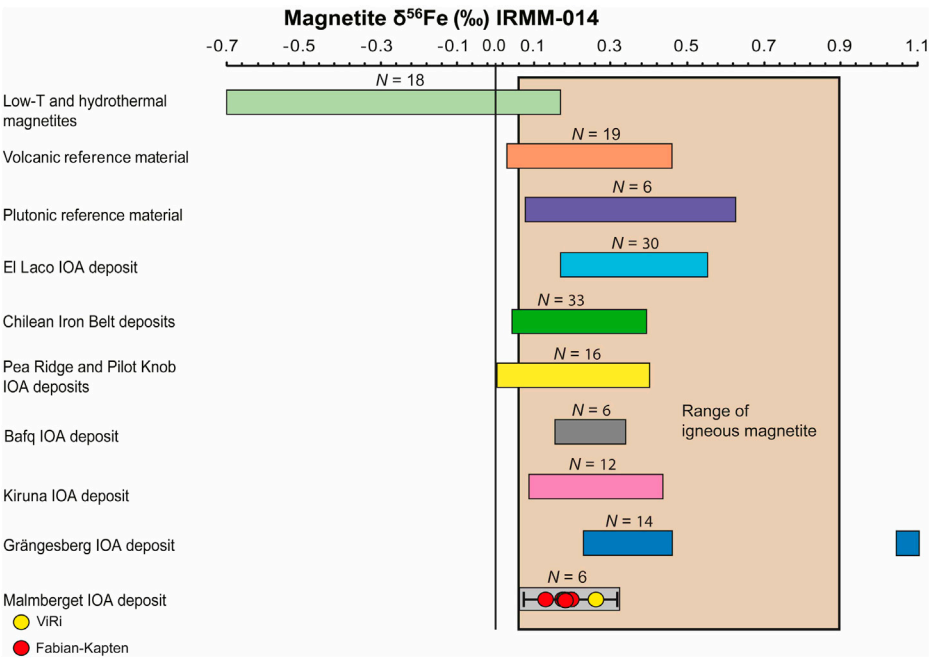

FIGURE 6 | Discriminant diagram for iron isotope signatures in magnetite. The coloured fields correspond to the reported range of $\delta^{56}Fe$ isotopes for magnetite reported in Bilenker et al. (2016), Childress et al. (2016), Troll et al. (2019), Rodriguez-Mustafa et al. (2020) and Xie et al. (2021). Range of igneous and hydrothermal magnetites from Anbar (2004), Heimann et al. (2008), Severmann and Anbar (2009), Wang et al. (2011), Sossi et al. (2012), Dziony et al. (2014), Bilenker et al. (2016).

DISCUSSION

Magnetite Textures

Ore and host rock in the Malmberget deposit show evident metamorphic recrystallisation (c.f. Geijer, 1930; Annersten, 1968; Lund, 2013; Bauer et al., 2018; Sarlus et al., 2020; Kambai, 2021; Yan et al., 2023a). Metamorphic textures in the magnetite ore include triple junctions and sub-grain domains (Geijer, 1930; Lund, 2013 Kambai, 2021; **Figure 2D**). However, our results indicate that the Malmberget deposit,

similar to IOA deposits globally, exhibits a magmatic to magmatic-hydrothermal Fe-O isotopic composition.

Magnetite Chemistry

Magnetite from the ViRi ore body exhibits elevated contents of trace elements such as Ti, V and Ga. Such element enrichment typically reflects magmatic processes at high temperatures and at comparably low oxygen fugacity (fO2 = FMQ + 0.2; Sievwright et al., 2017; Palma et al., 2021). In contrast, the Fabian-Kapten ore body displays elevated contents of Mn and Mg, which in melt-partitioning experiments has been attributed to an increase in oxygen fugacity from +0.2 to +3.7 relative to the fayalite-magnetite-quartz buffer (Sievwright et al., 2017).

Differences in trace element contents were further evaluated using magnetite trace element discrimination diagrams (Dupuis and Beaudoin, 2011). Although these diagrams are not considered suitable for global comparisons or as temperature proxies, they are useful to investigate deposit-scale variations (cf. Tornos et al., 2024). On a deposit-scale, all 24 data points plot within the igneous field in the Ti vs. V diagram (**Figure 4A**), mainly within the overlap zone between the igneous field and the hydrothermal field (n = 18). In the Al + Mn vs. Ti + V discriminatory diagram (Dupuis and Beaudoin, 2011), our sample suite span four fields (**Figure 4B**), namely, IOCG (n = 5), Kiruna-type (n = 13), Porphyry (n = 2) and ultramafic to mafic associated Fe-V, Ti (n = 4).

When investigating the distinct ore bodies, we note that the Fabian-Kapten and ViRi magnetite samples are separated into distinct groups in both the Ti vs. V plot and the Ti + V vs. Al + Mn discrimination diagram. The grouping in the Ti vs. V diagram is due to the uniform V contents in the magnetite across each respective ore body (**Figures 3**, **4**). In the Al + Mn vs. Ti + V discriminatory diagram, the Fabian-Kapten magnetite mainly plots at the boundary between Kiruna field and the IOCG field indicating a less pronounced magmatic character, and the ViRi magnetite data plot in the Kiruna-type field and the purely magmatic Fe-Ti, V field. In all, the trace elements exhibit a less-pronounced magmatic character for the Fabian-Kapten ore body compared to the ViRi ore body. These differences in magnetite trace element contents observed in magnetite from the Fabian-Kapten and ViRi ore bodies, with relatively elevated concentrations of elements associated with magmatic processes in the ViRi magnetite, indicates different ore sources or different proximities to the centre of the ore-forming system.

Magnetite Fe-O Isotopes

All the investigated magnetite samples from the Fabian-Kapten and ViRi ore bodies show magmatic to magmatic-hydrothermal Fe-O signatures, although the magnetite-source equilibrium calculations indicate the possibility of different sources and/or formation temperatures for the two ore bodies addressed in our study (**Supplementary Table S3**). For the Fabian-Kapten magnetite samples, uniform equilibrium between the magnetite and a potential source is only attained for high-temperature magmatic fluids. In contrast, calculations for the magnetite from the ViRi ore body satisfy equilibrium conditions with a magma of intermediate to mildly felsic composition.

Both $\delta^{18}O$ and $\delta^{56}Fe$ isotope values overlap with the established literature ranges for igneous magnetite that range from +1.0‰ to +4.0‰ for $\delta^{18}O$ values (Taylor, 1967; Loewen and Bindeman, 2016), and from +0.06‰ to +0.49‰ for $\delta^{56}Fe$ values (Heimann et al., 2008; Sossi et al., 2012; Dziony et al., 2014). Although the Fe-O isotope signatures of the massive magnetite samples from the Malmberget IOA deposits are principally magmatic, the ore forming medium, i.e., magma versus high-temperature hydrothermal fluid, remains unclear without assessing the full geological context.

Using available literature data for Fe-O isotopes from different types of magmas or high-temperature fluids, we conducted equilibrium calculations to better evaluate the precise magnetite source(s) for the Malmberget samples that we have investigated (**Supplementary Table S2**). These calculations were previously reported in the first author's MSc thesis and a conference contribution (Henriksson, 2022; Henriksson et al., 2023). The Malmberget IOA deposit is considered comagmatic to the mildly alkaline Kiirunavaara group metavolcanic rocks and their intrusive counterpart, the Perthite monzonite suite (Witschard, 1984; Frietsch and Perdahl, 1995; Martinsson and Perdahl, 1995; Sarlus et al., 2020). Potential magnetite sources thus include subduction zone related basaltic to dacitic magmas (900˚C) and magmatic high-temperature fluids (800˚C). Subduction related magmas of basalt to dacite composition have established $\delta^{18}O$ isotope values between +5.7‰ and +8.8‰, and $\delta^{56}Fe$-values between 0.00‰ and +0.12‰ (Heimann et al., 2008; Troll et al., 2019; Bindeman et al., 2022). Literature $\delta^{18}O$ equilibrium fractionation factors between potential sources and magnetite are established at −3.4‰ for basalt, at −4.0‰ for andesite, −4.3‰ for dacite, and at −5.3‰ for a high-temperature fluid (Zheng, 1991; Zhao and Zheng, 2003), whereas equilibrated $\delta^{56}Fe$ isotopic fractionation factors between these potential sources and magnetite are established at 0.03‰ for an intermediate to mildly felsic magma and at +0.24‰ for a high-temperature fluid (Heimann et al., 2008; Severmann and Anbar, 2009).

For $\delta^{18}O$ values, three out of the six samples satisfy equilibrium conditions with a basaltic magma, five with an andesitic magma, and five samples with a dacitic magma. In addition, all six samples show equilibrium with a high-temperature magmatic fluid (≤800˚C).

All samples have $\delta^{56}Fe$ values that are in equilibrium with a magmatic source, whereas all samples except ViRi-01 are also in equilibrium with a high-temperature fluid source. Consequently, equilibrium for the Fabian-Kapten magnetite samples indicates that the samples may have crystallised from magma but could also have formed from a high-temperature magmatic fluid source. In turn, the ViRi magnetite sample is not in equilibrium with a high-temperature fluid source and thus formed from a dacitic to andesitic magma.

Preservation of magmatic Fe-O signatures in IOA deposits despite greenschist to lower amphibolite facies

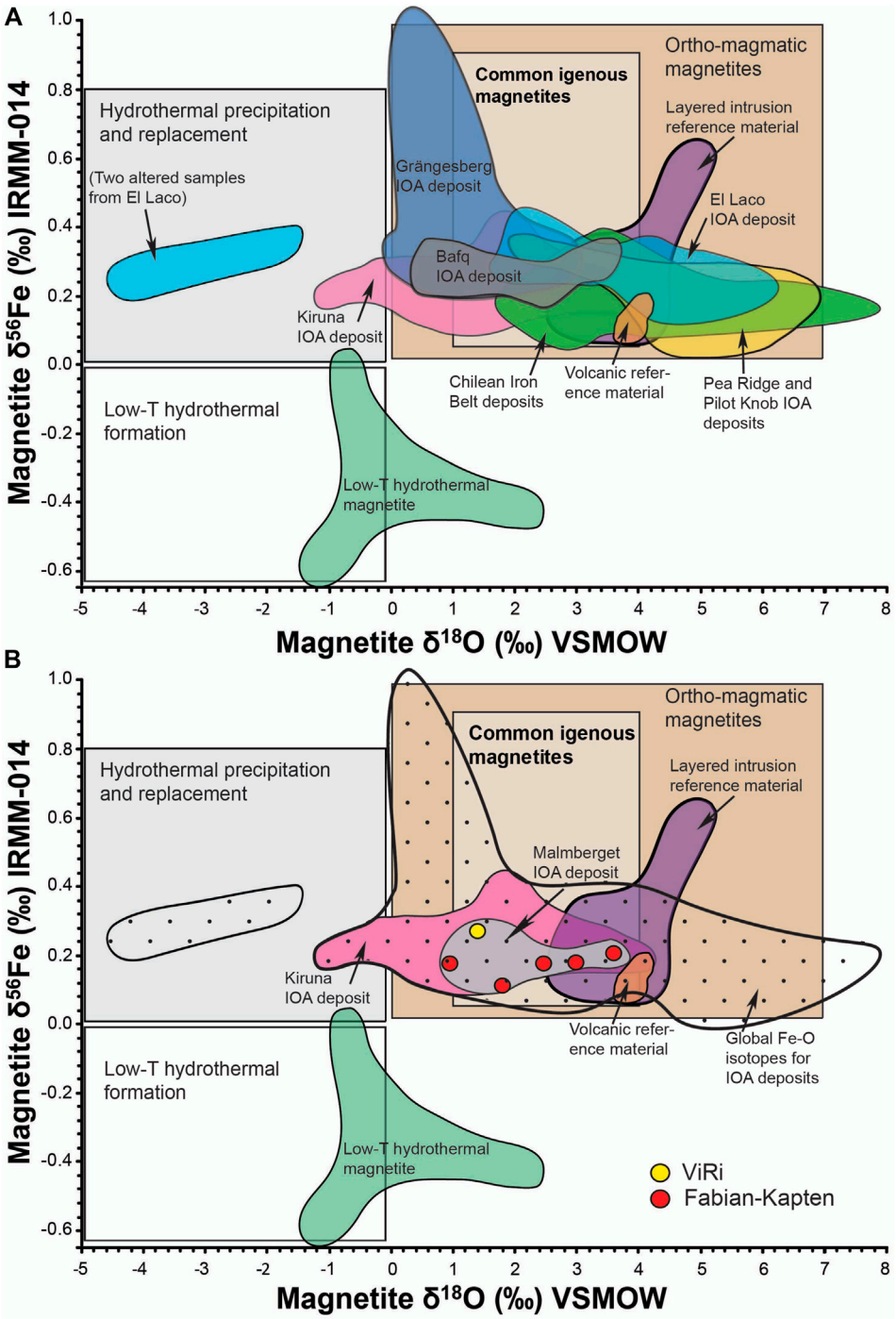

FIGURE 7 | Discriminatory diagram for magnetite based on $\delta^{18}O$ isotopes and $\delta^{56}Fe$ isotopes. **(A)** shows global IOA deposits, and intrusive, volcanic and low temperature hydrothermal reference samples **(B)** shows the fields for low temperature hydrothermal magnetite, the Kiruna IOA deposit, and global Fe-O isotopes for IOA deposits correspond to the distribution of values reported in Bilenker et al. (2016), Childress et al. (2016), Troll et al. (2019), Rodriguez-Mustafa et al. (2020) and Xie et al. (2021). Note that only data with coupled Fe-O isotopes is included.

metamorphism has previously been demonstrated for the deposits in the Kiruna area and also for the Grängesberg Mining District in south central Sweden (Jonsson et al., 2013; Troll et al., 2019; Yan et al., 2023b). At Grängesberg and Malmberget, the preservation of the Fe-O signature is attributed to the chemically and mechanically refractory properties of magnetite, in combination with the sheer tonnage of magnetite in IOA systems that self-buffer

against full replacement by later external fluids. The analysed massive magnetite samples from the Malmberget IOA deposit exhibit distinct equilibrated granoblastic textures with ubiquitous triple junctions, indicating high-grade (amphibolite facies) metamorphism (Annersten, 1968; **Figures 2A–D**). Metamorphic conditions are constrained by element distribution of ferromagnesian silicates in the presence of magnetite and hematite, homogenised apatite, and the presence of sillimanite-bearing parageneses and suggest peak metamorphic temperatures around 550˚C (Annersten, 1968; Lund, 2013; Chew and Spikings, 2015; Yan et al., 2023a). Regardless of the evident recrystallisation, all six analysed massive magnetite samples investigated preserve magmatic Fe-O isotope signatures and thus indicate a considerable degree of robustness to Fe-O isotope resetting (e.g., Troll et al., 2019; Reich et al., 2022) when investigating magnetite sources in large and metamorphically modified ore deposits. We acknowledge that eventual local hydrothermal isotope signatures or crystal-scale hydrothermal rims likely equilibrated during metamorphic recrystallisation. However, the primary magmatic isotope signature of the Malmberget deposit remains. This suggests that Fe-O systematics may be used to fingerprint the magnetite source(s) for IOA deposits that have recrystallised in metamorphic events, allowing us to 'see through' metamorphic effects to establish primary magmatic versus hydrothermal origins.

Wider Implications for Genesis of IOA Deposits

Recent development of coupled Fe-O isotope tracer studies (**Figure 7**) suggested that IOA deposits in China, Chile, Iran, Sweden, and the USA originate primarily from magmatic processes (cf. Simon et al., 2018; Troll et al., 2019; Majidi et al., 2021; Reich et al., 2022). Hydrothermal features and isotope signatures do occur, but are usually attributable to a progressive cooling of these magmatic systems and/or localised hydrothermal alteration and should not be confused with the primary, magmatic IOA ore forming processes (cf. Jonsson et al., 2013; Troll et al., 2019). The Fe-O isotopes of the Malmberget deposit are in concordance with these global findings, and suggest that the Malmberget, like most other IOA deposits, are primarily of magmatic origin.

On a deposit scale, however, trace element contents and Fe-O isotopes suggest chemical differences between the ViRi and Fabian-Kapten ore body. Although the Fe-O data from ViRi are limited, the Malmberget IOA deposit is widely considered as one ore-forming system (Geijer, 1930; Lund, 2013; Bauer et al., 2018), so two fundamentally different ore-sources are unlikely. Instead, we argue that the distinct trace element signatures and the observed Fe-O magnetite-source difference can be explained by the ore bodies' respective stratigraphic position and their proximity to the centre of the ore-forming magmatic system. Both trace element concentrations and Fe-O isotope correlations indicate that the ViRi ore body represents a purely magmatic (>800˚C) portion of the ore system that was proximal to the centre of the heat source of the ore-forming system. In contrast, the trace element concentrations and Fe-O isotope correlations in the Fabian-Kapten ore body show a less pronounced magmatic character (~800˚C), and may represent a more distal part of the ore-forming system. Our preliminary explanation of the differences in magnetite geochemistry is consistent with the different stratigraphic positions of these sub deposits in Malmberget as proposed by Bauer et al. (2018), but will require future in-depth testing on a deposit scale, using a larger sample suite that includes additional ore bodies.

In addition, the trace element and Fe-O isotope composition of the magnetite in the other ore bodies in the Malmberget IOA deposit are still unknown and an expanded high-resolution trace element and Fe-O isotope study would contribute significantly to a better understanding of internal relationships and detailed affinities between the different ore bodies in the Malmberget IOA deposit. This is especially important to better understand the geological history of the chemically distinct massive magnetite in the Western field and in the Printzsköld-Alliansen ore bodies. Both the Western field and Printzsköld-Alliansen ore bodies are geometrically controlled by deposit-scale, ore body-parallel shear-zones and are located close to the Lina granite-pegmatite intrusion suite, bordering the deposit to the north and northwest (Lund, 2013; Bauer et al., 2018 and references therein). Expelled fluids from the Lina granite-pegmatite intrusion combined with shear-zone related hydrothermal fluids could have caused a different, or partly modified Fe-O isotope composition of the massive magnetite in those areas. Recognition of different stratigraphic positions of the various sub-units of the ore deposit will likely help to further unravel the deformational history of the Malmberget IOA deposit and aid future exploration efforts in the area. On a provincial scale, the Fe-O isotopes from the Malmberget magnetite samples overlap with the world-famous Kiruna deposits, as established in Troll et al. (2019), which further emphasises the similarities between the Malmberget and the Kiruna IOA deposits. This may be indicative of a similar range of processes in the wider province and does not rule out the possibility of a single source at depth, which has been discussed in the context of a co-magmatic relationship between the IOA deposits as part of the emplacement of the regional Perthite monzonite suite-Kiirunavaara group rocks (Frietsch and Perdahl, 1995; Sarlus et al., 2018, 2020).

CONCLUSION

The Malmberget IOA ores have recrystallised during post-emplacement metamorphic processes, but the Fe-O isotope signature of the ore still preserved evidence for a primary magmatic to high-temperature magmatic-hydrothermal origin. The results from this study underline the robustness of Fe-O isotopes to fingerprint dominant magnetite source(s) of IOA deposits, even after moderate to considerable metamorphic overprinting of the deposits after primary formation. In a global context, the results from this study support the observation that IOA ores in Sweden, similar to younger examples in Chile, Iran and United States, are primarily of magmatic to magmatic-hydrothermal origin and form in a volcanic to sub-volcanic

environment at high-temperature. On a deposit scale, the recorded trace element contents and Fe-O isotope systematics in this study indicate a discrepancy between the ViRi and the Fabian-Kapten ore bodies in the Malmberget IOA deposit, which may be the result of different stratigraphic positions and distance from the centre, and thus the primary heat source of the ore-forming system. Further trace element and Fe-O isotope analysis of the remaining ore bodies in the Malmberget IOA deposit may contribute to a better understanding of the origin, eventual modifications, and internal stratigraphic relationships of this massive magnetite ore system.

DATA AVAILABILITY STATEMENT

The original contributions presented in the study are included in the article/**Supplementary Material**, further inquiries can be directed to the corresponding author.

AUTHOR CONTRIBUTIONS

VT and JH designed the concept of the study. TN, EK, and IB facilitated the analysis. VT, JH, TN, EK, IB, and TB interpreted the results. All authors participated in writing of the manuscript, working on a draft produced by JH and VT.

FUNDING

The authors declare that financial support was received for the research, authorship, and/or publication of this article. VT financed the research through funding from Swedish Research Council (Vetenskapsrådet grant number 2020-03789) and from European Research Council synergy grant (ERC-2023-SyG101118491). We further acknowledge the Swedish Research Council (Vetenskapsrådet) for financial support to the NordSIMS-Vegacenter national research infrastructure (grant number 2021-00276).

CONFLICT OF INTEREST

The authors declare that the research was conducted in the absence of any commercial or financial relationships that could be construed as a potential conflict of interest.

ACKNOWLEDGMENTS

We thank Albertus Smith for editorial handling. Comments from Shengchao Yan and an anonymous journal reviewer improved the quality of the manuscript. We thank Ulf B. Andersson, Jan-Anders Perdahl, Ian Cope, Karin Högdahl, Frances Deegan, Stefan Peters, Adam Simon and Vaida Kirkliauskaite for helpful comments on our work. Gavin Kenny and Andreas Karlsson at the Swedish Museum of Natural History are thanked for their assistance during EBSD analysis. Monika Hawrylak and Dimitra Antoniou are thanked for helping prepare **Figure 7**. This is Vegacenter publication #80. The Fe and O isotopes have been previously reported in the MSc thesis of JH (Henriksson, 2022) and have been presented at SGA, AGU and Nordic Geological Winter Meeting conferences previously (Henriksson et al., 2023; Troll et al., 2023; Troll et al., 2024).

SUPPLEMENTARY MATERIAL

The Supplementary Material for this article can be found online at: https://www.escubed.org/articles/10.3389/esss.2024.10126/full#supplementary-material

REFERENCES

Anbar, A. D. (2004). Iron Stable Isotopes: Beyond Biosignatures. *Earth Planet. Sci. Lett.* 217, 223–236. doi:10.1016/S0012-821X(03)00572-7

Andersson, J. B. H., Bauer, T. E., and Martinsson, O. (2021). Structural Evolution of the Central Kiruna Area, Northern Norrbotten, Sweden: Implications on the Geologic Setting Generating Iron Oxide-Apatite and Epigenetic Iron and Copper Sulfides. *Econ. Geol.* 116, 1981–2009. doi:10.5382/econgeo.4844

Andersson, U. B. (1991). Granitoid Episodes and Mafic-Felsic Magma Interaction in the Svecofennian of the Fennoscandian Shield, With Main Emphasis on the ~1.8 Ga Plutonics. *Precambrian Res.* 51, 127–149. doi:10.1016/0301-9268(91)90097-T

Annersten, H. (1968). A Mineral Chemical Study of a Metamorphosed Iron Formation in Northern Sweden. *Lithos* 1, 374–397. doi:10.1016/S0024-4937(68)80016-7

Bauer, T. E., Andersson, J. B. H., Sarlus, Z., Lund, C., and Kearney, T. (2018). Structural Controls on the Setting, Shape, and Hydrothermal Alteration of the Malmberget Iron Oxide-Apatite Deposit, Northern Sweden. *Econ. Geol.* 133, 377–395. doi:10.5382/econgeo.2018.4554

Bauer, T. E., Lynch, E. P., Sarlus, Z., Drejing-Carroll, D., Martinsson, O., Metzger, N., et al. (2022). Structural Controls on Iron Oxide-Copper-Gold Mineralization and Related Alteration in a Paleoproterozoic Supracrustal Belt: Insights From the Nautanen Deformation Zone and Surroundings, Northern Sweden. *Econ. Geol.* 117, 327–359. doi:10.5382/econgeo.4862

Bergman, S., Kübler, L., and Martinsson, O. (2001). *Description of Regional Geological and Geophysical Maps of Northern Norrbotten County (East of the Caledonian Orogen)*, 56. Serie Ba: Geological Survey of Sweden, 5–100. Available at: SGU.

Bergman, S., and Weihed, P. (2020). "Chapter 3 Archean (>2.6 Ga) and Paleoproterozoic (2.5–1.8 Ga), Pre- and Syn-Orogenic Magmatism, Sedimentation and Mineralization in the Norrbotten and Overkalix Lithotectonic Units, Svecokarelian Orogen," in *Sweden: Lithotectonic Framework, Tectonic Evolution and Mineral Resources*, ed. M. B. Stephens and J. Bergman Weihed, (London: Memoirs of the Geological Society), 50, 27–82. doi:10.1144/m50-2016-29

Bilenker, L. D., Simon, A. C., Reich, M., Lundstrom, C. C., Gajos, N., Bindeman, I., et al. (2016). Fe–O Stable Isotope Pairs Elucidate a High-Temperature Origin of Chilean Iron Oxide-Apatite Deposits. *Geochimica Cosmochimica Acta* 177, 94–104. doi:10.1016/j.gca.2016.01.009

Bindeman, I. N., Ionov, D. A., Tollan, P. M. E., and Golovin, A. V. (2022). Oxygen Isotope (δ18O, ∆′17O) Insights Into Continental Mantle Evolution Since the Archean. *Nat. Commun.* 13, 3779. doi:10.1038/s41467-022-31586-9

Borrok, D. M., Wanty, R. B., Ridley, W. I., Wolf, R., Lamothe, P. J., and Adams, M. (2007). Separation of Copper, Iron, and Zinc From Complex Aqueous Solutions for Isotopic Measurement. *Chem. Geol.* 242, 400–414. doi:10.1016/j.chemgeo.2007.04.004

Brand, W. A., Coplen, T. B., Vogl, J., Rosner, M., and Prohaska, T. (2014). Assessment of International Reference Materials for Isotope-Ratio Analysis (IUPAC Technical Report). *Pure Appl. Chem.* 86, 425–467. doi:10.1515/pac-2013-1023

Chew, D. M., and Spikings, R. A. (2015). Geochronology and Thermochronology Using Apatite: Time and Temperature, Lower Crust to Surface. *Elements* 11, 189–194. doi:10.2113/gselements.11.3.189

Childress, T., Simon, A. C., Day, W. C., Lundstrom, C. C., and Bindeman, I. N. (2016). Iron and Oxygen Isotope Signatures of the Pea Ridge and Pilot Knob Magnetite-Apatite Deposits, Southeast Missouri, USA. *Econ. Geol.* 111, 2033–2044. doi:10.2113/econgeo.111.8.2033

Childress, T., Simon, A. C., Reich, M., Barra, F., Bilenker, L. D., La Cruz, N. L., et al. (2020). Triple Oxygen (δ18O, ∆17O), Hydrogen (δ2H), and Iron (δ56Fe) Stable Isotope Signatures Indicate a Silicate Magma Source and Magmatic-Hydrothermal Genesis for Magnetite Orebodies at El Laco, Chile. *Econ. Geol.* 115, 1519–1536. doi:10.5382/econgeo.4760

Dare, S. A. S., Barnes, S., and Beaudoin, G. (2014). Did the Massive Magnetite "Lava Flows" of El Laco (Chile) Form by Magmatic or Hydrothermal Processes? New Constraints From Magnetite Composition by LAICP-MS. *Miner. deposita* 50, 607–617. doi:10.1007/s00126-014-0560-1

Duan, C., Li, Y., Mao, J., Hou, K., Wang, C., Yang, B., et al. (2019). Ore formation at the Washan iron oxide–apatite deposit in the Ningwu Ore district, eastern China: insights from in situ LA-ICP-MS magnetite trace element geochemistry. *Ore Geology Reviews* 112, 103064, ISSN 0169-1368. doi:10.1016/j.oregeorev.2019.103064

Dupuis, C., and Beaudoin, G. (2011). Discriminant Diagrams for Iron Oxide Trace Element Fingerprinting of Mineral Deposit Types. *Miner. Deposita* 46, 319–335. doi:10.1007/s00126-011-0334-y

Dziony, W., Horn, I., Lattard, D., Koepke, J., Steinhoefel, G., Schuessler, J. A., et al. (2014). *In-Situ* Fe Isotope Ratio Determination in Fe–Ti Oxides and Sulfides From Drilled Gabbros and Basalt From the IODP Hole 1256D in the Eastern Equatorial Pacific. *Chem. Geol.* 363, 101–113. doi:10.1016/j.chemgeo.2013.10.035

Frietsch, R., and Perdahl, J.-A. (1995). Rare Earth Elements in Apatite and Magnetite in Kiruna-Type Iron Ores and Some Other Iron Ore Types. *Ore Geol. Rev.* 9, 489–510. doi:10.1016/0169-1368(94)00015-G

Gaál, G., and Gorbatschev, R. (1987). An Outline of the Precambrian Evolution of the Baltic Shield. *Precambrian Res.* 64, 15–52. doi:10.1016/0301-9268(87)90044-1

Geijer, P. (1910). "Igneous Rocks and Iron Ores of Kiirunavaara, Luossavaara and Tuollavaara," in *Scientific and Practical Researches in Lapland Arranged by the Luossavaara-Kiirunavaara Aktiebolag, Geology of the Kiruna District 2*. Stockholm, 278.

Geijer, P. (1930). Gällivare Malmfält: Geologisk Beskrivning. *Sveriges Geol. Undersokning, C* 22, 115.

Hanski, E., and Huhma, H. (2005). "Central Lapland Greenstone Belt," in *The Precambrian Geology of Finland—Key to the Evolution of the Fennoscandian Shield*. Editors M. Lehtinen, P. A. Nurmi, and O. T. Rämo (Elsevier), 139–193. doi:10.1016/S0166-2635(05)80005-2

Heimann, A., Beard, B. L., and Johnson, C. M. (2008). The Role of Volatile Exsolution and Sub-Solidus Fluid/Rock Interactions in Producing High 56Fe/54Fe Ratios in Siliceous Igneous Rocks. *Geochimica Cosmochimica Acta* 72, 4379–4396. doi:10.1016/j.gca.2008.06.009

Henriksson, J. S. (2022). EBSD Investigation of High-Temperature Magnetite From Apatite-Iron-Oxide Deposits: Implications for the Formation of Giant Kiruna-Type Deposits. MSc thesis. Uppsala, Sweden: Uppsala University.

Henriksson, J. S., Troll, V. R., Kooijman, E., and Bindeman, I. N. (2023). "Fe-O Isotope Systematics and Magnetite Chemistry of the Malmberget Iron-Oxide Apatite Deposit, Sweden," in Abstract Proceedings 17th SGA Biennial Meeting, Zürich, Switzerland, August 28–September 1, 2023 1, 354–357.

Hildebrand, R. S. (1986). Kiruna-Type Deposits; Their Origin and Relationship to Intermediate Subvolcanic Plutons in the Great Bear Magmatic Zone, Northwest Canada. *Econ. Geol.* 81, 640–659. doi:10.2113/gsecongeo.81.3.640

Hitzman, M. W., Oreskes, N., and Einaudi, M. T. (1992). Geological Characteristics and Tectonic Setting of Proterozoic Iron Oxide (Cu-U-Au-REE) Deposits. *Precambrian Res.* 58, 241–287. doi:10.1016/0301-9268(92)90121-4

Högdahl, K., Andersson, U. B., and Eklund, O. (2004). *The Transscandinavian Igneous Belt (TIB) in Sweden: A Review of Its Character and Evolution*, 37. Espoo, Finland: Geological Survey of Finland Special Paper, 125.

Jochum, K. P., Willbold, M., Raczek, I., Stoll, B., and Herwig, K. (2005). Chemical Characterisation of the USGS Reference Glasses GSA-1G, GSC-1G, GSD-1G, GSE-1G, BCR-2G, BHVO-2G and BIR-1G Using EPMA, ID-TIMS, ID-ICP-MS and LA-ICP-MS. *Geostand. Geoanalytical Res.* 29, 285–302. doi:10.1111/j.1751-908X.2005.tb00901.x

Jonsson, E., Harlov, D., Majka, J., Högdahl, K., and Persson-Nilsson, K. (2016). Fluorapatite-Monazite-Allanite Relations in the Grängesberg Apatite-Iron Oxide Ore District, Bergslagen, Sweden. *Am. Mineralogist* 101, 1769–1782. doi:10.2138/am-2016-5655

Jonsson, E., Troll, V. R., Högdahl, K., Harris, C., Weis, F. A., Persson-Nilsson, K., et al. (2013). Magmatic Origin of Giant "Kiruna-type" Apatite-Iron-Oxide Ores in Central Sweden. *Sci. Rep.* 3, 1644. doi:10.1038/srep01644

Kambai, K. (2021). Geochemical Understanding of Vanadium in Malmberget Ores (Kiruna-Type), Northern Sweden. MSc Thesis. Luleå, Sweden: Luleå University of Technology.

Kenny, G. G., Mänttäri, I., Schemider, M., Whitehouse, M. J., Nemchin, A. A., Belluci, J. J., et al. (2020). Age of Sääksjärvi Impact Structure, Finland: Reconciling the Timing of Small Impacts in Crystalline Basement With Regional Basin Development. *J. Geol. Soc.* 177, 1231–1243. doi:10.1144/jgs2020-034

Knipping, J. L., Bilenker, L. D., Simon, A. C., Reich, M., Barra, F., Deditius, A. P., et al. (2015). Giant Kiruna-Type Deposits Form by Efficient Flotation of Magmatic Magnetite Suspensions. *Geology* 43, 591–594. doi:10.1130/G36650.1

LKAB (2024). *LKAB Mineral Resources Summary Report December 2023 (PERC)*. Luleå, Sweden: LKAB. Available at: https://lkab.mediaflowportal.com/documents/folder/231556/ (Accessed March 29, 2024).

Loewen, M., and Bindeman, I. N. (2016). Oxygen Isotope Thermometry Reveals High Magmatic Temperatures and Short Residence Times in Yellowstone and Other Hot-Dry Rhyolites Compared to Cold-Wet Systems. *Am. Mineralogist* 101, 1222–1227. doi:10.2138/am-2016-5591

Lund, C. (2013). Mineralogical, Chemical and Textural Characterization of the Malmberget Iron Ore Deposit for a Geometallurgical Model. PhD Thesis. Luleå, Sweden: Luleå University of Technology.

Lund, J. (2014). A Lithogeochmical Study of Northern Sweden and the Kiruna and Malmberget Iron-Apatite Ore Deposits. MSc Thesis. Uppsala, Sweden: Uppsala University.

Majidi, S. A., Omrani, J., Troll, V. R., Weis, F. A., Houshmandzadeh, A., Ashouri, E., et al. (2021). Employing Geochemistry and Geochronology to Unravel Genesis and Tectonic Setting of Iron Oxide-Apatite Deposits of the Bafq-Saghand Metallogenic Belt, Central Iran. *Int. J. Earth Sci.* 110, 127–164. doi:10.1007/s00531-020-01942-5

Martinsson, O. (1997). Tectonic Setting and Metallogeny of the Kiruna Greenstones. PhD Thesis. Luleå, Sweden: Luleå University of Technology.

Martinsson, O., Billström, K., Broman, C., Weihed, P., and Wanhainen, C. (2016). Metallogeny of the Northern Norrbotten Ore Province, Northern Fennoscandian Shield With Emphasis on IOCG and Apatite-Iron Ore Deposits. *Ore Geol. Rev.* 78, 447–492. doi:10.1016/j.oregeorev.2016.02.011

Martinsson, O., and Perdahl, J.-A. (1995). "Paleoproterozoic Extensional and Compressional Magmatism in Northern Sweden," in *Svecofennian Volcanism in Northern Sweden*. Editor J.-A. Perdahl (Luleå University of Technology). PhD Thesis.

Millet, M. A., Baker, J. A., and Payne, C. E. (2012). Ultra-Precise Stable Fe Isotope Measurements by High Resolution Multiple-Collector Inductively Coupled Plasma Mass Spectrometry With a Fe-57-Fe-58 Double Spike. *Chem. Geol.* 304, 18–25. doi:10.1016/j.chemgeo.2012.01.021

Nadoll, P., Angerer, T., Mauk, J. L., French, D., and Walshe, J. (2014). The Chemistry of Hydrothermal Magnetite: A Review. *Ore Geol. Rev.* 61, 1–32. doi:10.1016/j.oregeorev.2013.12.013

Naslund, H. R. (1983). The Effect of Oxygen Fugacity on Liquid Immiscibility in Iron-Bearing Silicate Melts. *Am. J. Sci.* 283, 1034–1059. doi:10.2475/ajs.283.10.1034

Naslund, H. R., Henríquez, F., Nyström, J. O., Vivallo, W., and Dobbs, F. M. (2002). "Magmatic Iron Ores and Associated Mineralisation: Examples From the High Andes and Coastal Cordillera," in *Hydrothermal Iron Oxide Copper-Gold and Related Deposits: A Global Perspective*. Editor T. M. Porter (Adelaide, Australia: PGC Publishing), 207–226.

Nyström, J. O., and Henríquez, F. (1994). Magmatic Features of Iron Ores From the Kiruna Type in Chile and Sweden: Ore Textures and Magnetite Geochemistry. *Econ. Geol.* 89, 820–839. doi:10.2113/gsecongeo.89.4.820

Ovalle, J. T., La Cruz, N. L., Reich, M., Barra, F., Simon, A. C., Konecke, B. A., et al. (2018). Formation of massive iron deposits linked to explosive volcanic eruptions. *Sci. Rep.* 8, 14855. doi:10.1038/s41598-018-33206-3

Palma, G., Reich, M., Barra, F., Ovalle, J. T., del Real, I., and Simon, A. C. (2021). Thermal Evolution of Andean Iron Oxide–Apatite (IOA) Deposits as Revealed by Magnetite Thermometry. *Sci. Rep.* 11, 18424. doi:10.1038/s41598-021-97883-3

Parák, T. (1975). Kiruna Iron Ores Are Not "Intrusive-Magmatic Ores of the Kiruna Type". *Econ. Geol.* 70, 1242–1258. doi:10.2113/gsecongeo.70.7.1242

Paton, C., Hellstrom, J., Paul, B., Woodhead, J., and Hergt, J. (2011). Iolite: Freeware for the Visualisation and Processing of Mass Spectrometric Data. *J. Anal. Atomic Spectrom.* 26, 2508. doi:10.1039/C1JA10172B

Peters, S. T. M., Alibabaie, N., Pack, A., McKibbin, S. J., Raeisi, D., Nayebi, N., et al. (2020). Triple Oxygen Isotope Variations in Magnetite From Iron-Oxide Deposits, Central Iran, Record Magmatic Fluid Interaction With Evaporite and Carbonate Host Rocks. *Geology* 48, 211–215. doi:10.1130/G46981.1

Pietruszka, D., Hanchar, J. M., Tornos, F., Whitehouse, M., and Velasco, R. F. (2024). Tracking Isotopic Sources of Immiscible Melts at the Enigmatic Magnetite-(Apatite) Deposit at El Laco, Chile, Using Pb Isotopes. *GSA Bull.* 136, 513–530. doi:10.1130/B36506.1

Pietruszka, D., Hanchar, J. M., Tornos, F., Wirth, R., Graham, N., Severin, K., et al. (2023). Magmatic Immiscibility and the Origin of Magnetite-(Apatite) Iron Deposits. *Nat. Commun.* 14, 8424. doi:10.1038/s41467-023-43655-8

Reich, M., Simon, A. C., Barra, F., Palma, G., Hou, T., and Bilenker, L. D. (2022). Formation of Iron Oxide-Apatite Deposits. *Nat. Rev. Earth and Environ.* 3, 758–775. doi:10.1038/s43017-022-00335-3

Rodriguez-Mustafa, M. A., Simon, A. C., del Real, I., Thompson, J. F. H., Bilenker, L. D., Barra, F., et al. (2020). A Continuum From Iron Oxide Copper-Gold to Iron Oxide-Apatite Deposits: Evidence From Fe and O Stable Isotopes and Trace Element Chemistry of Magnetite. *Econ. Geol.* 115, 1443–1459. doi:10.5382/econgeo.4752

Romer, R. L. (1996). U-Pb systematics of stilbite-bearing low-temperature mineral assemblages from the Malmberget iron ore, northern Sweden. *Geochemica et Cosmochimica Acta* 60, 1951–1961.

Salazar, E., Barra, F., Reich, M., Simon, A. C., Leisen, M., Palma-Lira, G., et al. (2020). Trace Element Geochemistry of Magnetite From the Cerro Negro Norte Iron Oxide–Apatite Deposit, Northern Chile. *Miner. Deposita* 55, 409–428. doi:10.1007/s00126-019-00879-3

Sarlus, Z., Andersson, U. B., Martinsson, O., Bauer, T. E., Wanhainen, C., Andersson, J. B. H., et al. (2020). Timing and Origin of the Host Rocks to the Malmberget Iron Oxide-Apatite Deposit, Sweden. *Precambrian Res.* 342, 105652. doi:10.1016/j.precamres.2020.105652

Sarlus, Z., Martinsson, O., Bauer, T. E., Wanhainen, C., Andersson, J. B. H., and Nordin, R. (2018). Character and Tectonic Setting of Plutonic Rocks in the Gällivare Area, Northern Norrbotten, Sweden. *GFF* 141, 1–20. doi:10.1080/11035897.2018.1526209

Severmann, S., and Anbar, A. D. (2009). Reconstructing Paleoredox Conditions Through a Multitracer Approach: The Key to the Past Is the Present. *Elements* 5, 359–364. doi:10.2113/gselements.5.6.359

SGU (2023). Statistics of the Swedish Mining Industry 2022. SGU Periodiska Publikationer: 2023, 1. Available at: https://resource.sgu.se/dokument/publikation/pp/pp202301rapport/pp2023-1-rapport.pdf. Accessed March 27, 2024.

Sievwright, R. H., Wilkinson, J. J., O'Niell, H.St. C., and Berry, A. J. (2017). Thermodynamic Controls on Element Partitioning Between Titanomagnetite and Andesitic-Dacitic Silicate Melts. *Contribution Mineralogy Petrology* 172, 62. doi:10.1007/s00410-017-1385-6

Simon, A. C., Knipping, J., Reich, M., Barra, F., Deditius, A. P., Bilenker, L., et al. (2018). "Kiruna-Type Iron Oxide-Apatite (IOA) and Iron Oxide Copper-Gold (IOCG) Deposits Form by a Combination of Igneous and Magmatic-Hydrothermal Processes: Evidence From the Chilean Iron Belt," in *Metals, Minerals, and Society*. Editors A. M. R. Arribas and J. L. Mauk (Littleton, United States: Society of Economic Geologists Special Publication), 21, 89–114. doi:10.5382/SP.21.06

Sossi, P. A., Foden, J. D., and Halverson, G. P. (2012). Redox-Controlled Iron Isotope Fractionation During Magmatic Differentiation: An Example From the Red Hill Intrusion, S. Tasmania. *Contrib. Mineral. Petrol.* 164, 757–772. doi:10.1007/s00410-012-0769-x

Taylor, H. P. (1967). "Oxygen Isotope Studies of Hydrothermal Mineral Deposits," in *Geochemistry of Hydrothermal Ore Deposits*. Editor H. L. Barnes (Holt, Rinehart and Winston Inc.), 109–142.

Toplis, M. J., and Corgne, A. (2002). An Experimental Study of Element Partitioning Between Magnetite, Clinopyroxene and Iron-Bearing Silicate Liquids With Particular Emphasis on Vanadium. *Contrib. Mineral. Petrol.* 144, 22–37. doi:10.1007/s00410-002-0382-5

Tornos, F., Hanchar, J. M., Steele-MacInnis, M., Crespo-Feo, E., Kamenetsky, V., and Casquet, C. (2024). Formation of Magnetite(-Apatite) Systems by Crysallizing Ultrabasic Iron-Rich Melts and Slag Separation. *Miner. Deposita*, 1–37. doi:10.1007/s00126-023-01203-w

Tornos, F., Velasco, F., and Hanchar, J. M. (2016). Iron-Rich Melts, Magmatic Magnetite, and Superheated Hydrothermal Systems: The El Laco Deposit, Chile. *Geology* 44, 427–430. doi:10.1130/G37705.1

Tornos, F., Velasco, F., and Hanchar, J. M. (2017). The Magmatic to Magmatic-Hydrothermal Evolution of the El Laco Deposit (Chile) and Its Implications for the Genesis of Magnetite-Apatite Deposits. *Econ. Geol.* 112, 1595–1628. doi:10.5382/econgeo.2017.4523

Troll, V. R., Henriksson, J. S., Kooijman, E., and Bindeman, I. N. (2023). "Origin and Affinities of the Malmberget Iron Oxide-Apatite Deposit, Northern Sweden: Insights From Fe-O Isotopes," in Abstract proceedings AGU23 fall meeting, San Francisco, CA, V43D–V0206.

Troll, V. R., Henriksson, J. S., Kooijman, E., and Bindeman, I. N. (2024). *Magnetite Chemistry and Fe-O Isotopes Help Unravel Origin and Affinities of the Malmberget Iron Oxide-Apatite Deposit, Northern Sweden*. Gothenburg, Sweden: Abstract Volume 36th Nordic Geological Winter Meeting, 131.

Troll, V. R., Weis, F. A., Jonsson, E., Andersson, U. B., Majidi, S. A., Högdahl, K., et al. (2019). Global Fe-O Isotope Correlation Reveals

Magmatic Origin of Kiruna-Type Apatite-Iron-Oxide Ores. *Nat. Commun.* 10, 1712. doi:10.1038/s41467-019-09244-4

U.S. Geological Survey (2023). *Mineral. Commod. Summ.* 2023, 210. doi:10.3133/mcs2023

Valley, J. W., Kitchen, N., Kohn, M. J., Niendorf, C. R., and Spicuzza, M. J. (1995). UWG-2, a Garnet Standard for Oxygen Isotope Ratios: Strategies for High Precision and Accuracy With Laser Heating. *Geochimica. Cosmochimica. Acta* 59, 5223–5231. doi:10.1016/0016-7037(95)00386-X

Wang, Y., Zhú, X., Mao, J., Li, Z., and Cheng, Y. (2011). Iron Isotope Fractionation During Skarn-Type Metallogeny: A Case Study of Xinqiao Cu-S-Fe-Au Deposit in the Middle-Lower Yangtze Valley. *Ore Geol. Rev.* 43, 194–202. doi:10.1016/j.oregeorev.2010.12.004

Wechsler, B. A., Lindsley, D. H., and Prewitt, C. T. (1984). Crystal Structure and Cation Distribution in Titanomagnetites (Fe3-xTixO4). *Am. Mineralogist* 69, 754–770.

Westhues, A., Hanchar, J. M., LeMessurier, M. J., and Whitehouse, M. J. (2017). Evidence for Hydrothermal Alteration and Source Regions for the Kiruna Iron Oxide–Apatite Ore (Northern Sweden) From Zircon Hf and O Isotopes. *Geology* 45, 571–574. doi:10.1130/G38894.1

Wen, G., Li, J. W., Hofstra, A. H., Koenig, A. E., Lowers, H. A., and Adams, D. (2017). Hydrothermal reequilibration of igneous magnetite in altered granitic plutons and its implications for magnetite classification schemes: insights from the Handan-Xingtai iron district, North China craton. *Geochimica et Cosmochimicha Acta* 213, 255–270. doi:10.1016/j.gca.2017.06.043

Witschard, F. (1984). The Geological and Tectonic Evolution of the Precambrian of Northern Sweden – A Case for Basement Reactivation? *Precambrian Res.* 23, 273–315. doi:10.1016/0301-9268(84)90047-0

Woodhead, J. D., Hellstrom, J., Hergt, J. M., Greig, A., and Maas, R. (2007). Isotopic and Elemental Imaging of Geological Materials by Laser Ablation Inductively Coupled Plasma-Mass Spectrometry. *Geostand. Geoanalytical Res.* 31, 331–343. doi:10.1111/j.1751-908X.2007.00104.x

Xie, Q. H., Zhang, Z. C., Campos, E., Deng, J., Cheng, Z., Fei, X., et al. (2021). Constraints of Fe-O Isotopes on the Origin of Magnetite in the El Laco Kiruna-Type Iron Deposit, Chile. *Ore Geol. Rev.* 130, 103967. doi:10.1016/j.oregeorev.2020.103967

Yan, S., and Liu, W. (2022). Rare Earth Elements in the Iron-Oxide Apatite (IOA) Deposit: Insights From Apatite. *Int. Geol. Rev.* 64, 3230–3247. doi:10.1080/00206814.2022.2028198

Yan, S., Wan, B., and Andersson, U. B. (2023a). Apatite Age and Composition: A Key to the Geological History of the Malmberget Iron-Oxide-Apatite (IOA) Deposit and the Region. *J. Geochem. Explor.* 252, 107267. doi:10.1016/j.gexplo.2023.107267

Yan, S., Wan, B., and Andersson, U. B. (2023b). Hydrothermal Circulation at 1.8 Ga in the Kiruna Area, Northern Sweden, as Revealed by Apatite Geochemical Systematics. *Precambrian Res.* 395, 107151. doi:10.1016/j.precamres.2023.107151

Ye, Z., Mao, J., Yang, C., Usca, J., and Li, X. (2023). Trace Elements in Magnetite and Origin of the Mariela Iron Oxide-Apatite Deposit, Southern Peru. *Minerals* 13, 934. doi:10.3390/min13070934

Zhao, Z. F., and Zheng, Y. F. (2003). Calculation of Oxygen Isotope Fractionation in Magmatic Rocks. *Chem. Geol.* 193, 59–80. doi:10.1016/S0009-2541(02)00226-7

Zheng, Y. F. (1991). Calculation of Oxygen Isotope Fractionation in Metal Oxides. *Chem. Geol.* 55, 2299–2307. doi:10.1016/0016-7037(91)90105-E